Available online at www.sciencedirect.com
ScienceDirect
Medical Engineering & Physics 29 (2007) 413–431
Medical Engineering & Physics
www.elsevier.com/locate/medengphy

Needle insertion into soft tissue: A survey

Niki Abolhassani [a,b,*], Rajni Patel [a,b,*], Mehrdad Moallem [a,b]

[a] *Canadian Surgical Technologies & Advanced Robotics (CSTAR), London, Ontario, Canada*
[b] *Department of Electrical & Computer Engineering, University of Western Ontario, London, Ontario, Canada*

Received 5 August 2005; received in revised form 26 June 2006; accepted 4 July 2006

Abstract

Needle insertion in soft tissue has attracted considerable attention in recent years due to its application in minimally invasive percutaneous procedures such as biopsies and brachytherapy. This paper presents a survey of the current state of research on needle insertion in soft tissue. It examines the topic from several aspects, e.g. modeling needle insertion forces, modeling tissue deformation and needle deflection during insertion, robot-assisted needle insertion, and the effect of different trajectories on tissue deformation. All studies show that the axial force of a needle during insertion in soft tissue is the summation of different forces distributed along the needle shaft such as stiffness force, frictional force and cutting force. Some studies have modeled these forces. The force data in some procedures is used for identifying tissue layers as the needle is inserted or for path planning. Needle deflection and tissue deformation are major problems for accurate needle insertion and attempts have been made to model them. Using current models several insertion techniques have been developed which are briefly reviewed in this paper.

Keywords: Needle insertion; Tissue deformation; Robot-assisted needle insertion; Modeling and simulation; Needle deflection; Needle steering; Trajectory generation

1. Introduction

1.1. Motivation

Many modern clinical practices involve percutaneous ("through the skin") diagnosis and local therapies. In these procedures, thin tubular devices (needles, catheters, tissue ablation probes, etc.) have to be inserted deep into soft, inhomogeneous tissue to reach a target. There are several applications for percutaneous needle insertion such as biopsies [1], regional anesthesia, blood sampling [2], neurosurgery [3] and brachytherapy [4]. The effectiveness of a treatment and the success or precision of a diagnosis is highly dependent on the accuracy of percutaneous insertion [5]. There is not a defined tolerance for the accuracy of needle insertion in clinical practice and in general, insertions with less needle misplacement result in more effective treatment [6] or increase the precision of diagnosis. The desired performance depends on the application. In procedures such as biopsy (for prostate, kidney, breast and liver), brachytherapy and anesthetic, placement accuracy of millimeters is required while in brain, fetus, eye and ear procedures placement accuracy of micro-millimeter is desirable. Clinical studies have revealed that targeting error (needle misplacement) may be due to imaging limitations, image misalignments, target uncertainty, human errors, target movement due to tissue deformation and needle deflection [7–12]. In Ref. [8], for imaging misalignment of ±5 mm in only one view, a targeting error of about 10 mm was calculated. In Ref. [11], post-implantation measurements showed that the prostate gland volume which was receiving the least prescribed dose was 20–30% due to tissue deformation and gland motion, i.e., an average misplacement of 6.5 mm where the prostate volume was in the range of 25–55 cm^3.

Furthermore, in a percutaneous procedure, the target might be in the millimeter neighborhood of another organ, vessel or nerve. Therefore, extra caution is required to avoid any damage or spread of a disease which in turn may lead

* Corresponding authors. Tel.: +1 519 663 3111; fax: +1 519 663 8401.
E-mail addresses: nabolhas@uwo.ca (N. Abolhassani), rajni@eng.uwo.ca (R. Patel).

1350-4533/$ – see front matter © 2006 IPEM. Published by Elsevier Ltd. All rights reserved.
doi:10.1016/j.medengphy.2006.07.003

to subsequent complications (e.g., seed migration) that may even be fatal [13]. Some of the desired accuracies may be achieved using current tools and models but accurate needle placement for many other applications requires much more research and development. Real-time visualization and high precision imaging techniques can increase the performance of the surgeon in navigating the tool and tracking the target [14]. Advanced mechanical tools that consider the constraints imposed by anatomy using haptic feedback and those that reduce or remove human errors due to fatigue, hand tremor and problems in hand/eye coordination can contribute to reduction in targeting error [7]. Medical simulators that can accurately model a clinical procedure are of great advantage for training medical residents, predicting the outcome of complex procedures and practicing new procedures. These simulators would reduce the need for animals, cadavers and anatomical phantoms as training objects and medical residents would have unlimited opportunity to practice before performing an operation on a patient.

1.2. Problem

Percutaneous therapies are constrained procedures where target visibility, target access and tool maneuverability in addition to physiological changes to the target are key issues. During some conventional needle insertion procedures, the surgeon relies on kinesthetic feedback from the tool (needle or catheter) and his or her mental 3D visualization of the anatomical structure [15]. Real-time imaging techniques that are used in some procedures can improve target visibility. However, human errors [13], imaging limitations, target uncertainty [8], tissue deformation and needle deflection [9] are a few known problems that contribute to needle misplacement in percutaneous procedures. Human errors may be related to poor techniques and insufficient skills of a physician. Target uncertainty may be caused by patient motion, physiological or geometry related problems [8]. Despite the availability of different imaging modalities to improve visualization; there are several factors such as high cost, poor resolution, probe availability, X-ray exposure, material compatibility, reliable real-time image processing techniques, etc. that may limit application of imaging in some clinical and research studies. A few examples of these limitations are: working with robots where MRI is the imaging modality (magnetic interference), using artificial phantoms when the imaging modality is ultrasound (acoustic properties), and using camera when performing *ex vivo* experiments (non-visibility of target). Needle deflection is generally due to the bevel tip and diameter of the needle [16,17]. The tissue, into which the needle is inserted, may also contribute to needle deflection. The factors that affect tissue deformation include mechanical properties of soft tissue, needle tip contact force, and frictional forces between the tissue and the needle shaft [11].

Other causes of inaccuracy in percutaneous therapies are physiological changes in the organ between the planning and treatment phases, glandular swelling during the operation, difference in tissue types involved in each procedure, differences in mechanical properties of healthy and diseased tissue, changes of mechanical properties when tissue is damaged and variability of soft tissue properties for the same organ in different patients.

1.3. Solution

To date, a number of researchers have explored ways to improve the process of needle insertion in soft tissue using robotics and medical imaging [18–22] in order to improve the accuracy of the procedure. Fig. 1 shows a schematic diagram of an image-guided robot-assisted percutaneous procedure.

Medical imaging (CT-scan, ultrasound, fluoroscopy, MRI) plays an important role in image-guided procedures and these procedures rely on powerful computer systems for navigating, planning, tracking and modeling. From several studies and clinical practices, it is known that off-line medical imaging does not provide enough accuracy for precise procedures. Therefore, real-time imaging techniques have been developed [23–25]. Image registration, image segmentation and augmented reality are the major topics in image-guided surgery. In Ref. [26], Peters reviewed different methods of imaging used in image-guided surgery including virtual reality. It should be mentioned that in the absence of real-time imaging, force feedback [27] and an accurate mechanical model which identifies tissue deformation and target movement would be valuable. Such models could be updated with real-time force feedback during needle insertion.

Simulation and modeling of needle insertion have been studied in 2D and 3D environments for general [15,28] or particular [24,29] applications. Boundary conditions, tissue geometry and biomechanical tissue properties are of major importance in simulation and modeling applications because these factors affect the amount of tissue deformation, needle deflection and interaction forces. Needle insertion has also been studied in the context of haptic rendering for simulation [30] and virtual reality systems for medical procedures [31,32]. Needle insertion with sensorless planning, respiratory motion simulation [33] and automatic targeting [34] are also topics that have attracted considerable research.

Robotic devices for percutaneous procedures have been discussed in reviews of medical robotics such as [35,36]. While a review of robotic devices or image-guided interventions for percutaneous procedures is not the aim of this paper, it is worth mentioning the work of a few groups in this area to show that this is also a fertile area of research into needle insertion. Krieger et al. [37] developed MR image-guided prostate interventions using an MR compatible manipulator with 3 degrees of freedom (DOF) and Susil et al. [38] demonstrated the feasibility and accuracy of needle placement, intra-prostatic injections and fiducial marker placements using the manipulator for operations on anesthetized canines. Fichtinger et al. [39] developed a robotically

assisted needle insertion system for prostate biopsy and therapy with intraoperative CT guidance. Schneider et al. [40] presented a robotic device for transrectal needle insertion into the prostate with integrated ultrasound. Ebrahimi et al. [41] introduced a hand-held steerable device which incorporates a pre-bent stylet inside a straight cannula, and Maurin et al. [42] presented a parallel robotic system for percutaneous procedures under CT guidance. Hong et al. [43] built an ultrasound-guided needle insertion robot. Their robot has a 5-DOF passive arm for positioning the needle at the skin entry point and 2-DOF for insertion. They developed a real-time image servo system to compensate for tissue deformation and organ movement.

1.4. Scope of this review

Fig. 2 shows different stages during the needle insertion procedure as reviewed in this paper. Studies that are reviewed have in general been undertaken to improve both manual and robotic percutaneous procedures. When a needle is inserted percutaneously, visual and haptic feedback are required to enhance the clinical operation. Visual and haptic data provide knowledge about tissue deformation and needle deflection during the needle insertion procedure and are useful in modeling. Visual data can also be processed and used in image-guided procedures. The models obtained from visual and haptic data can be used for intraoperative path planning and trajectory generation and they can also be used for better off-line planning and simulation for medical training. For deep needle insertion, knowledge of anatomical structures is also a requirement. In manual procedures, the knowledge and expertise can be integrated with visual feedback from an imaging modality to guide the needle with a limited accuracy. In robotic procedures, imaging data is incorporated with precise robotic motion and accurate prediction of needle deflection and tissue deformation to increase the accuracy of the overall procedure.

This paper is intended to give an overview of recent non-clinical work in the field of needle insertion in soft tissue with a focus on the effect of force measurements for modeling the needle–tissue interaction and on guiding robots to improve the precision of needle insertion (shaded area in Fig. 2). Knowing interaction forces and developing appropriate needle deflection and tissue deformation models during needle insertion are the key issues for accurate insertion. This paper reviews those studies that implicitly improve the needle inser-

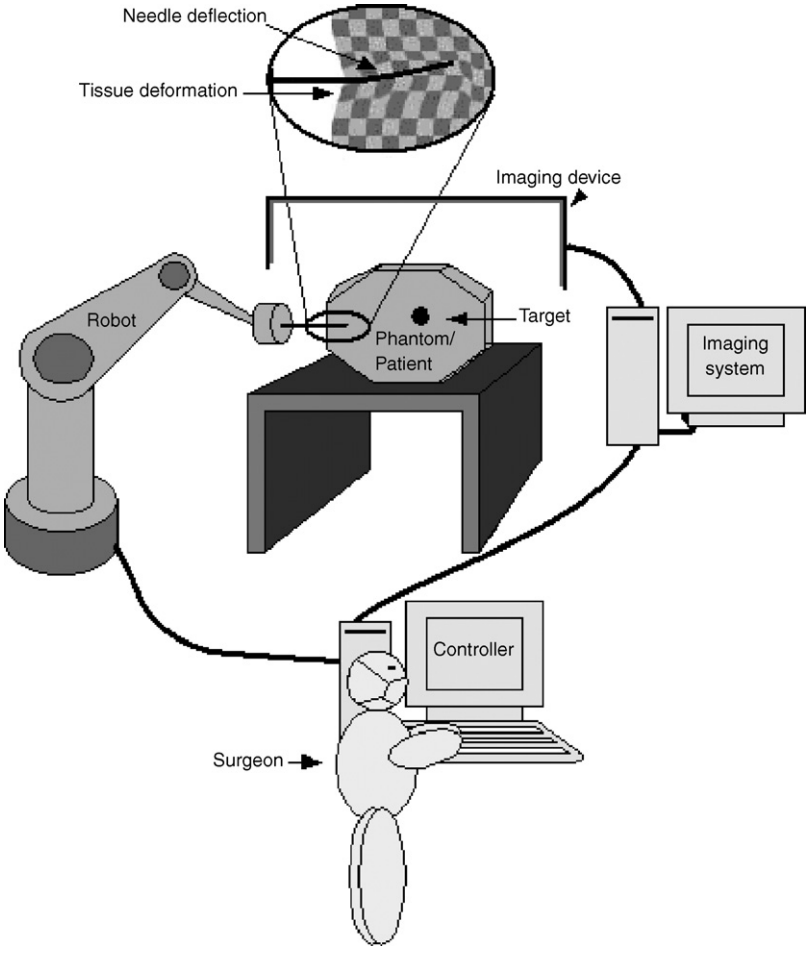

Fig. 1. Schematic diagram of robotic needle insertion.

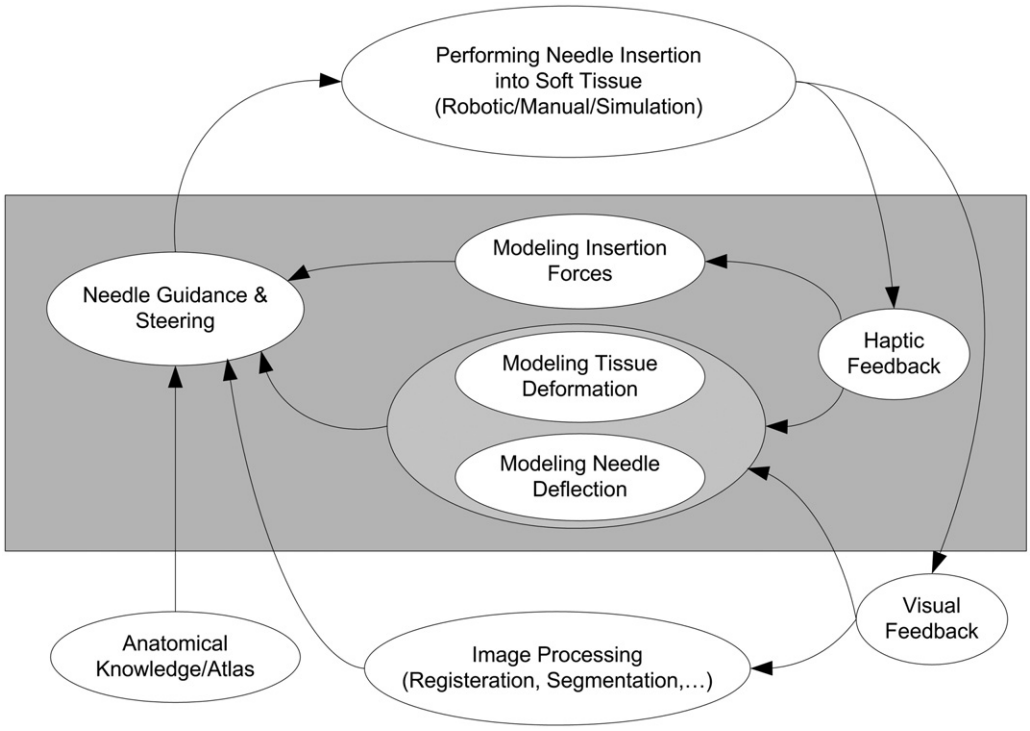

Fig. 2. Block diagram of needle insertion procedure. The gray area is in the scope of this paper.

tion procedure for both manual and robot-assisted, image-guided procedures as well as simulation systems for medical training. However, a review of robotic systems, imaging techniques and simulation systems developed for percutaneous procedures is not included in this paper. The performance of each study can be evaluated based on the verification of the results with an imaging system or supporting the experimental results with an analytical model. It is clear that those results and models that are based on experiments with an artificial phantom should be validated with *ex vivo* and *in vivo* experiments.

This paper is organized as follows. First an overview of interaction forces during needle insertion is presented. Second, modeling and simulation of tissue deformation are discussed. It should be noted that the requirements for tissue modeling vary slightly depending on applications. Third, the effect of needle deflection on accurate insertion is reviewed. Fourth, some publications on trajectory planning and insertion techniques for needle insertion in manual and robot-assisted insertion are discussed. In this section, we also look into force measurement for precise control of needle insertion. Finally, challenges in this field of research as well as concluding remarks are presented. Figs. 3 and 4 illustrate some of the terms used in this paper.

2. Modeling needle insertion forces

Knowledge of interactive forces during needle insertion plays an important role in precise needle insertion. This knowledge can help to identify and model different tissue types and it can also provide feedback for precise control of robot-assisted insertion while reducing tissue deformation and needle deflection. In general, an accurate model for insertion forces should be able to identify features such as

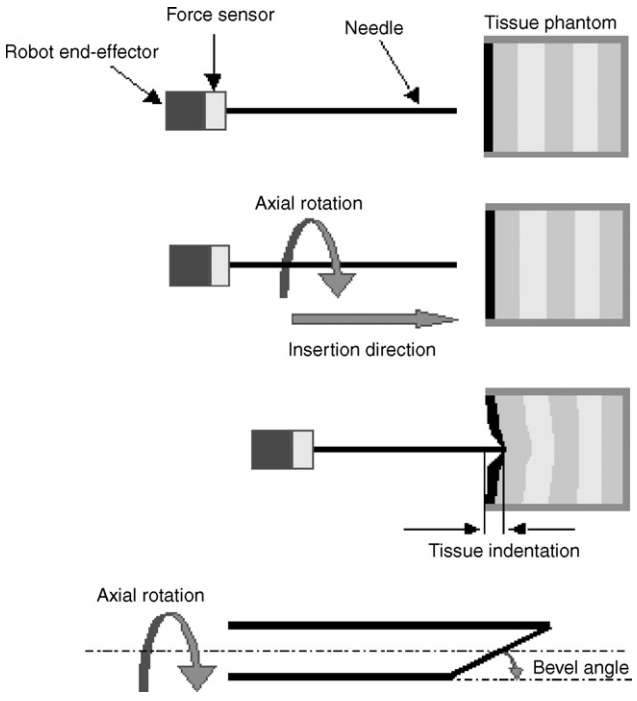

Fig. 3. Schematic definitions of some terms used in the text.

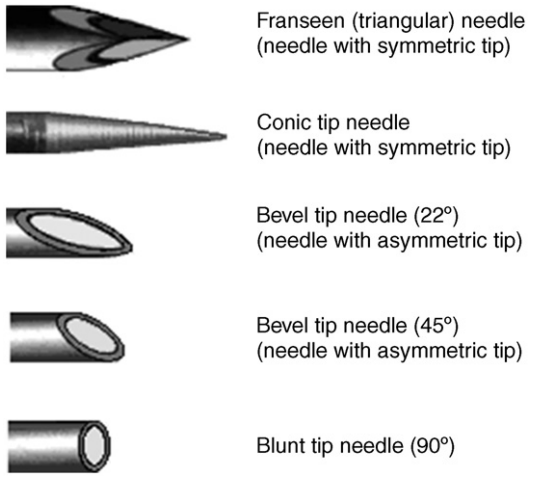

Fig. 4. Needles with different tips.

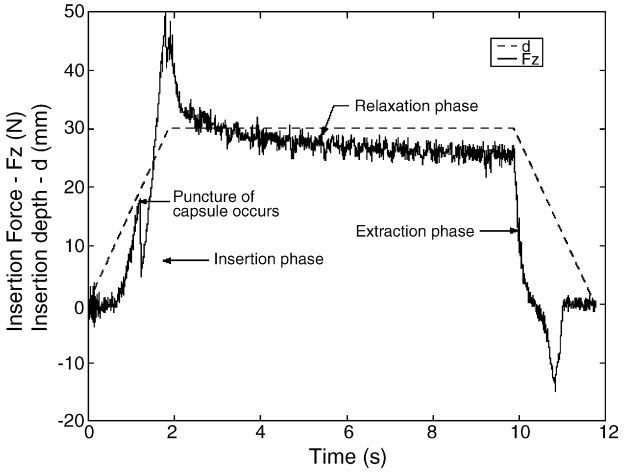

Fig. 5. Needle insertion with direct access to the liver [45] (courtesy of B. Maurin, LSIIT, Illkrich, France).

the force peak, latency in the force changes, and separation of different forces such as stiffness and damping force. It is also desirable for the model to calculate the magnitude of the insertion force such that it matches the actual measurements. For applications with predictive force control, a tolerance in the magnitude or latency of the force measurements may not be acceptable while in simulations systems where haptic tools are used, such tolerance could be related to human perception (0.5 N in magnitude [44]).

In percutaneous therapies, the needle punctures[1] and passes through different tissue layers such as skin, muscle, fatty and connective tissue. Puncturing and cutting through each of these layers requires different amounts of force. The amount of force even varies from patient to patient for the same tissue type due to prior treatments, age, gender, body mass, etc. Fig. 5 shows the force profile with respect to time during needle insertion and retraction [45]. This data is obtained from *in vivo* insertion into liver when other anatomical layers have been removed.

Simone and Okamura [46] investigated modeling of needle insertion forces for bovine liver and considered puncture of the capsule as an event which divides the insertion to pre-puncture and post-puncture phases. In pre-puncture, the force increases steadily and a sharp drop in the amount of force identifies the puncture event. During post-puncture, the amount of force is variable due to friction, cutting and collision with interior structures. The total force acting on the needle is

$$f_{\text{needle}}(z) = f_{\text{cutting}}(z) + f_{\text{friction}}(z) + f_{\text{stiffness}}(z) \tag{1}$$

where z is the position of the needle tip. In (1) the stiffness force belongs to pre-puncture and the friction and cutting forces belong to post-puncture. Pre-puncture and post-puncture phases are shown in Fig. 6. The stiffness force is due to the elastic properties of the organ and its capsule. Simone and Okamura [46] modeled the stiffness force using a nonlinear spring model:

$$f_{\text{stiffness}} = \begin{cases} 0 & z < z_1 \\ a_1 z + a_2 z^2 & z_1 \le z \le z_2 \\ 0 & z > z_3 \end{cases} \tag{2}$$

where z is the needle tip position and z_1, z_2 and z_3 are shown in Fig. 6. The friction was modeled by a modified Karnopp model [48] (see Fig. 7):

$$f_{\text{friction}} = \begin{cases} C_{\text{n}}\,\text{sgn}(\dot{z}) + b_{\text{n}}\dot{z} & \dot{z} \le -\Delta v/2 \\ \max(D_{\text{n}}, F_{\text{a}}) & -\Delta v/2 < \dot{z} \le 0 \\ \min(D_{\text{p}}, F_{\text{a}}) & 0 < \dot{z} < \Delta v/2 \\ C_{\text{p}}\,\text{sgn}(\dot{z}) + b_{\text{p}}\dot{z} & \dot{z} \ge \Delta v/2 \end{cases} \tag{3}$$

where C_{n} and C_{p} are negative and positive values of dynamic friction, b_{n} and b_{p} negative and positive damping coefficients and D_{n} and D_{p} negative and positive values of static friction, $\dot{z}$ the relative velocity between the needle and tissue, $\Delta v/2$ the value below which the velocity is considered to be zero and F_{a} is the sum of nonfrictional forces applied to the system. In Ref. [46], Simone and Okamura performed sinusoidal needle insertions with different frequencies and

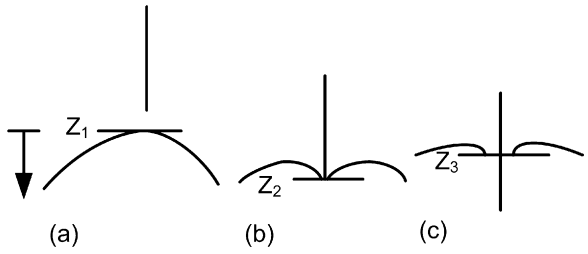

Fig. 6. Locations of the tissue surface at different stages of needle insertion: (a) pre-puncture, (b) puncture, and (c) post-puncture [47] (courtesy of C. Simone, Johns Hopkins University, MD, USA).

[1] The term "puncturing" refers to making a hole in the outer layer of a tissue using the tip of a needle and the term "cutting" refers to piercing the inner layers of the tissue after puncture and during penetration of the needle into the tissue.

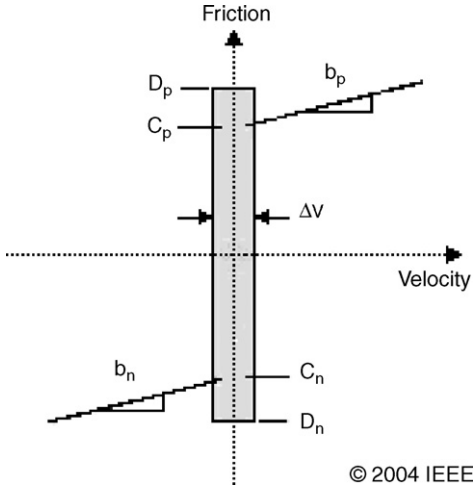

Fig. 7. The modified Karnopp friction model [48,49].

velocities to obtain force data and find the model parameters. They modeled the remaining forces as the cutting forces which are necessary for slicing through the tissue. The cutting forces were modeled as constants for a given tissue:

$$f_{\text{cutting}} = \begin{cases} 0 & z_{\text{tip}} \le z_2, t < t_{\text{p}} \\ a & z_{\text{tip}} > z_3, t \ge t_{\text{p}} \end{cases} \quad (4)$$

where z, z_2, z_3 are the same as in (2), t is time and t_{p} is the time of puncture. The cutting force value was calculated by subtracting the estimated friction force from the total force after puncture. CT fluoro imaging was used to identify different phases and calculate the relative velocities of the tissue and the needle. A MATLAB program was used to find the model parameters for the average data obtained during needle insertion into bovine liver. They validated their model by comparing it with actual data. Fig. 8 shows a comparison between the above needle insertion model and two insertions in an excised bovine liver. The overall shape is similar. However, there is a large discrepancy between their model and the actual data at the moment of puncture. They have assumed that the discrepancy is due to the wide variations in liver geometry and its internal structure. However, even for tissues with simpler structures the model may not closely match for different patients. Therefore, more care should be taken when using such a model for motion control. In Ref. [49], Okamura et al. investigated the effect of needle diameter and tip type on insertion forces. They found a significant effect of tip type on insertion forces. Insertion forces increased as the needle tip type changed from triangular to bevel and bevel to cone but the bevel angle did not affect the axial force significantly. They also found that for each of the tip types, the increase of needle diameter increased the insertion force.

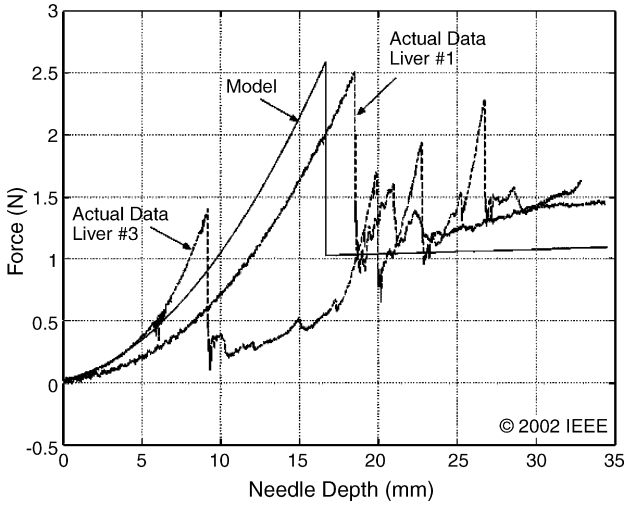

Fig. 8. Comparison of the needle insertion model with two insertions in bovine liver [46].

Maurin et al. [45] studied insertion forces during *in vivo* needle insertions into liver and kidney of anesthetized pigs. They compared manual and robotic insertions. In the manual insertions, the radiologist inserted a needle by manually holding the force device attached to the needle. In the robotic insertions, the needle holder was attached to the end-effector of a robot. They did not use an imaging system, therefore in the manual insertion the depth was hard to estimate and the needle was inserted for approximately 30–50 mm while in robotic insertion they had a fixed insertion depth of 20 mm. They had two methods for accessing the organ: "direct access" (all other anatomical layers were removed) and "with skin access" (the needle passed through different anatomical layers). From their result, it can be seen that multiple layers in the method "with skin access" accentuate the forces. Also in their results, robotic insertion in general required less force than manual insertion in the method "with skin access"; however, such conclusion cannot be generalized for their result of the "direct access" method. To compare the amount of peak force in manual and robotic insertions, a controlled insertion depth is a key factor which was not considered. They also used two models for their measurements. The first model was taken from Simone and Okamura [46]. They fitted a second-order polynomial to the data for modeling stiffness force and the Karnopp model for the friction force. The second model was taken from Maurel [50] and based on the work of Fung [51]. Their modeling showed low errors for both models (see Fig. 9).

Using a specially developed seven-axis load cell (see Fig. 10) for measuring and separating forces during needle insertion, Kataoka et al. [52] performed experiments on an exposed prostate of a defrosted beagle cadaver. They used a needle with a triangular pyramid tip. Three different forces acting on the needle were measured independently: the tip force, the friction force and the clamping force. The tip force acting on the needle tip in the axial direction was assumed to be primarily related to cutting. The shape of the needle tip affects the magnitude of this force. The friction force acting on the sidewall of the needle shaft in the axial direction was considered to be the summation of Coulomb and viscous friction. The clamping force acting on the sidewall of the needle shaft in the normal direction was taken to be the

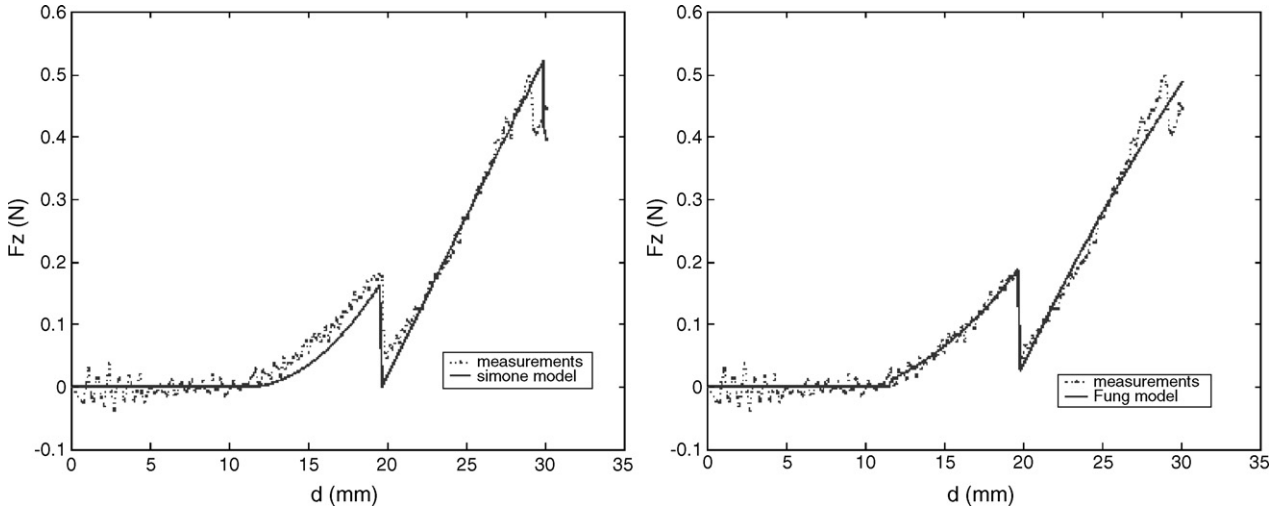

Fig. 9. Two models fitted with data from *in vivo* needle insertions (left: Simone and Okamura and right: Maurel) [45] (courtesy of B. Maurin, LSIIT, Illkrich, France).

resistance force of the tissue due to its compression away from the needle path. The clamping force increases as the needle is inserted into the tissue. The magnitude is affected by the needle gauge and the incision shape. They also found that the tip force decreases right after puncture to the value for the cutting force, which is a constant. This decrease occurs because the prostate capsule is harder than the inner tissue. However, generalizing constant cutting force for all tissue types may not be sufficiently accurate. The friction force increases proportionally to the true insertion depth according to the needle diameter. Kataoka et al. [52] showed that the true insertion depth can be calculated by subtracting the surface motion (indentation) from the driving distance of the needle. This cannot be an accurate calculation because during penetration not only does the tissue deform and compress but the surface also tends to slide back on the needle after puncture. They presented that the total axial force is the summation of the tip force and the friction force. The clamping force affects the value of the friction force.

Matsumiya et al. [53] presented an experimental study of robotic needle insertion into a formaldehyde-fixed (FA-fixed) human vertebra and measured forces and torques during insertion. They used a needle with triangular pyramid tip and a robot developed for percutaneous vertebroplasty, which could insert the needle with bidirectional axial rotation. Their results showed a strong correlation between the axial force variation during insertion and the distribution of the bone local CT-value along the needle path. In their study, the influence of FA-fixation on the axial force was investigated by measuring and comparing the axial force during needle insertion to human femoral heads that had been preserved under freezing or FA-fixation. The axial force during robotic insertion into human femoral head was found to be smaller than that during manual insertion (about 1/3 of the manual insertion). They mentioned two reasons for the smaller axial force in robotic insertion. First, the robot can hold the needle more stably during insertion than a human (the speed of insertion in their experiments was less than 1 mm/s). Second, the speed and the angle of rotation (in case of having axial rotation) can be varied easily in robotic insertion. They concluded that the use of robotics can contribute to safer needle insertion in percutaneous vertebroplasty because of reduction in the amount of axial force in robotic insertion. This is based on the clinical observation but it requires an analytical support.

DiMaio and Salcudean [15,54] explored the relationship between needle forces and 2D tissue deformation using a planar robot (pantograph), an artificial tissue phantom (made of PVC) and a CCD camera. Fig. 11 illustrates the force distribution along the needle shaft [15]. This distribution indicates the existence of two forces: an axial friction force between the needle and the tissue, which is uniform along the shaft, and a

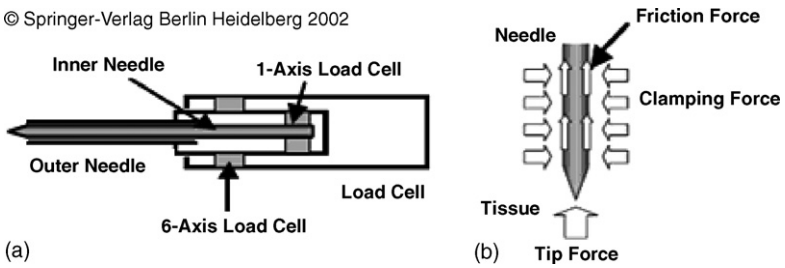

Fig. 10. (a) Structure of the seven-axis load cell and (b) the forces acting on a needle inside the tissue [52].

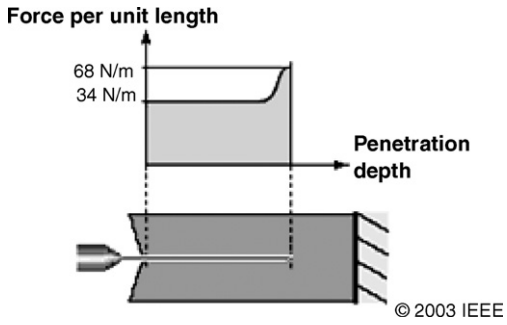

Fig. 11. Estimated needle force distribution (insertion velocity is 1 mm/s). This distribution is taken from the estimated tissue phantom forces at nodes along the needle shaft [15].

force peak at the needle tip, which results from the cutting of the tissue and is approximately twice the friction force [15]. DiMaio and Salcudean showed that during penetration the shaft force increases with insertion velocity while the force peak at the distal end of the needle appears to be somewhat independent of velocity, becoming less prominent at higher velocities. Their study is useful for preliminary simulations; however, needle insertion in such artificial tissue phantoms cannot help to realistically model interactive forces during needle insertion in inhomogeneous, viscoelastic tissue. The results of all the above studies agree with the model presented by Simone and Okamura [46].

Podder et al. [55] performed the first *in vivo* force/torque measurement for manual needle insertion in human soft tissue. They equipped a hand-held adapter with a 6-DOF force/torque sensor and a 6-DOF electromagnetic position sensor. They measured force, torque and position during manual needle insertion in a prostate brachytherapy procedure. They also performed *in vitro* needle insertions into beef steak wrapped with chicken skin using a 6-DOF robot. The results of their *in vivo* experiments show that the average maximum insertion force was about 15 N for the perineum, about 7 N for the prostate and the resultant transverse force was about 1.6 N. Their *in vivo* results for manual needle insertion should be very useful for designing robotic tools and simulators for needle insertion.

3. Modeling tissue deformation during needle insertion

Tissue deformation and tissue modeling are complex because of the inhomogeneous, nonlinear, anisotropic, elastic and viscous behavior of soft tissue. Real-time and accurate calculation of such behavior could significantly improve robotic percutaneous therapy, surgical planning and simulation systems for medical training. Hence, tissue modeling is the subject of much research.

Physical and mathematical tools are being developed to accurately model soft tissue. For modeling soft tissue, it is necessary to determine the biomechanical properties through *in vitro* and *in vivo* measurements, use constitutive laws and develop spring-mass or finite element (FE) models for real-time simulations [56].

3.1. Biomechanical properties of soft tissue

There are many articles on the mechanical properties of biological tissue systems and *in vitro* measurement of soft tissues [51,57,58]; however recent studies are focused on obtaining quantitative information on the biomechanical properties of *in vivo* soft tissue. Ultrasonic methods have been developed for measuring biomechanical properties of soft tissue. Nightingale et al. [59] investigated acoustic remote palpation imaging for measuring tissue stiffness. Trahey et al. [60] developed acoustic radiation force impulse imaging for measuring arterial stiffness. Han et al. [61] introduced a prototype ultrasound indentation system to compare various methods for measuring *in vivo* biomechanical properties. Menciassi et al. [62] presented a smart robotic micro-instrument for measuring *in vivo* tissue properties, both qualitatively and quantitatively. Their device also sensed micro-vessels on the basis of pulsating fluid flowing through them. Ottensmeyer et al. [63] performed four categories of experiments for measuring viscoelastic properties of soft tissue: *in vivo*, *in vitro* excised lobe case, *ex vivo* whole organ with perfusion and *ex vivo* whole organ without perfusion. Two different measurement devices were used. They used the TeMPeST (tissue measurement property sampling tools) instrument [64] for measuring the compliance of solid organ tissues *in vivo* by performing small-indentation test on suitable structures (such as liver, kidney). TeMPeST 1-D (for measuring the small strain frequency response of tissue) has a 5 mm circular punch that vibrates the tissue while recording applied load and relative displacement at the rate of 200 Hz, depending on the tissue. Its range of motion is 1 mm and can exert forces up to 300 mN. Ottensmeyer et al. [63] also used VESPI (visco-elastic soft-tissue property indentation instrument) for similar experiments. VESPI is designed for measuring normal tissue indentation (measuring the large strain time-domain response) and has a 6 mm flat punch that rests on the tissue surface until a standard mass is released on it. Loads from 20 to 100 g can create a large range of motion. They also build an apparatus similar in concept to the normothermic extracorporeal liver perfusion system in order to maintain cellular integrity during *ex vivo* experiments. In their experiments with the perfusion apparatus, the large deformation time responses approached those of tissues tested *in vivo*. They also found that testing whole organ provides a more accurate reference than cut specimen. Although the perfusion system offers many advantageous over *in vivo* experiments such as reducing the cost of testing, ethical and administrative issues, it does not consider any anatomical structures surrounding the organ which could change the boundary conditions.

Brouwer et al. [65] developed devices for measuring tissue extension, tissue indentation and instrument–tissue interaction forces. They performed *ex vivo* and *in vivo* experiments

on abdominal porcine tissue and modeled the collected data with exponential equations. Preconditioning was performed on tissue for *ex vivo* experiments. However, the results are not discussed in sufficient details. It is not known from the paper if the results of *in vivo* and *ex vivo* experiments belong to the organ of one pig or not. It should also be mentioned that in this work the tissue was cut from its surrounding anatomical structure for *ex vivo* experiments.

Brown et al. [66] used a motorized endoscopic grasper to perform *in vivo* and *in situ* experiments on abdominal porcine tissue and applied cyclic and static compressive loadings. They did not perform any preconditioning on the tissues. They found that the relaxation behavior after the first squeeze is exponential and modeled the stress–strain data with exponential equations. However, a tendency to a linear model was observed in the relaxation behavior of subsequent squeezes. Also the relaxation behavior was shown to be different between *in vivo* and *in situ* experiments. It is valuable that in this work both *in vivo* and *in situ* experiments are performed on the organ of the same pig.

Kerdok et al. [67,68] proposed building a database of physical standards for measuring soft tissue deformation. They investigated the deformation of a cube of soft polymer that is referred to as the "truth cube". They placed beads in a grid pattern throughout the volume of the cube. The displacement of the beads was measured using CT-scan images when the cube was under pressure. Boundary conditions, material properties and bead displacement were used to compare the performance of real-time modeling of deformation using finite element method (FEM) with deformation of the truth cube. This preliminary work found the tradeoff between the accuracy of FEM versus its computational cost. Kerdok et al. [67] concluded that due to the uncertain accuracy and difficulty of implementing FEM techniques that can deal with gross deformation, truth cube was a better method for validating real-time soft tissue simulation models. In Ref. [67], the cube was made of silicon rubber which does not behave like real soft tissue, and had a simple geometry which is not the case in real organs. Therefore, as the next step of this study, Kerdok et al. [68] and Howe [69] replaced the truth cube by a whole real organ (excised bovine liver). The liver organ was perfused with physiological solutions at pressures and temperatures mimicking *in vivo* circulatory conditions. The relaxation modulus and creep modulus were measured and constitutive law parameters that result in accurate FEM were calculated. They showed that their setup maintained the *in vivo* mechanical responses of liver.

3.2. Development of tissue models for needle insertion

It should be mentioned that soft tissue constitutive laws that affect tissue modeling are based on nonlinear stress–strain relationships, large deformations, visco-elasticity, nonhomogeneity, and anisotropy [56]. The nonlinear stress–strain relationship results in force not being linearly proportional to displacement. Large deformations may cause geometric nonlinearties [70]. Visco-elasticity, nonhomogeneity and anisotropy, respectively, mean that soft tissue properties are functions of time, they vary throughout tissue thickness and they vary with direction. To date, there is no closed-form solution for a majority of these problems [56]. Mass-spring and finite element models are the current solutions for modeling tissue deformation. Mass-spring models may work well in real-time but they have limited accuracy [68]. On the other side, FEM is accurate for modeling small linear elastic deformation but FEM calculations are expensive with respect to time and FEM accuracy is very much dependent to its inputs [68,71].

DiMaio and Salcudean [15,54,72,73] have done extensive studies on simulation of tissue deformations that occur during needle insertion in soft tissue. They developed a real-time haptic simulation system. Their system allowed the user to experience both visual and kinesthetic feedback while executing a virtual planar needle insertion. Considering linear elastostatic models for soft tissue, tissue deformation is described using FEM as

$$K\underline{u} = \underline{f} \tag{5}$$

where K is the system stiffness matrix, $\underline{u}$ and $\underline{f}$ are displacement and force vectors for nodes lying on the finite element mesh. In Ref. [54] the force boundary conditions were only applied to the nodes in direct contact with the needle shaft, and deformation was calculated only for those working nodes. Displacement boundary conditions in this simulation constrained tissue nodes to the needle geometry and varied for rigid and flexible needles in their model. Displacement boundary conditions for a flexible needle and force boundary conditions were calculated from physical experiments. The response of their system was pre-computed by means of condensation [74]. According to Nienhuys and van der Stappen [28,75], using a uniform mesh which is necessary for condensation occupies a large amount of memory and is computationally intensive. To overcome this problem for 2D and 3D simulation of nonlinear material models using FEM, Nienhuys and van der Stappen presented a solution based on iterative algorithms which do not require pre-computed structures. This implies that the mesh can be refined adaptively in the region of interest with low computational requirements. They mentioned that "the computational cost of a 3D simulation is too high for haptic applications". They did not consider needle deflection in their simulation.

Alterovitz et al. [29,76,77] presented 2D FE modeling and simulation of needle insertion with application to prostate brachytherapy. Their FE models of soft tissue approximate the prostate, its membrane and the surrounding fatty tissue as linearly elastic homogenous materials. The mechanical properties such as Young's modulus and Poisson's ratio were set using the results of [78]. Needle insertion forces were applied as boundary conditions on the elements. It was assumed that puncturing membrane tissue requires additional force at the needle tip. In their simulation [76], a node was maintained at

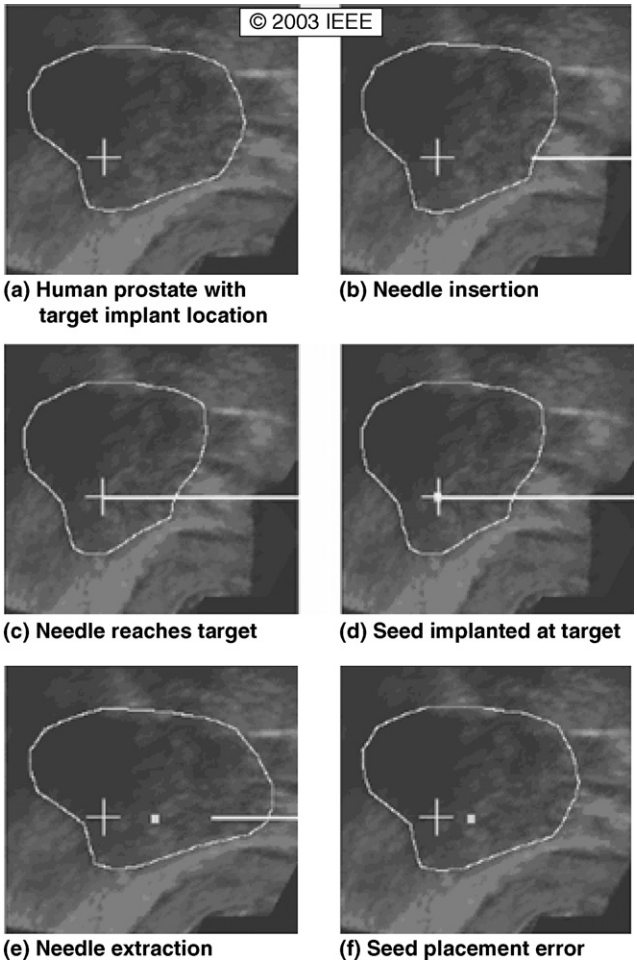

Fig. 12. (a) Outline of the prostate and the target implant location (white cross). (b) When the needle is inserted through soft tissue and pushes against the prostate membrane, the tissue compresses. The force on the needle increases until the prostate membrane is punctured. (c) The needle moves deeper into the prostate and stops when it is estimated that the tip of the needle is at the target location. Stopping the needle causes the tissue to reach a stable state. (d) A radioactive seed is deposited in the tissue at the needle tip. (e) The needle is retracted. (f) The tissue containing the implanted seed returns to its equilibrium state after the needle is completely withdrawn from the tissue. The placement error, the distance between the target and the resulting seed location, is the result of tissue deformation during these phases [29,76].

the needle tip during insertion for applying the tip force, and a list of nodes along the needle shaft (that are constrained to move horizontally) were maintained for friction forces. In the simulation, a static ultrasound image was deformed using the generated mesh deformations. In the simulation, they considered the effects of tissue deformation during seed implantation, which lead to imprecise seed placement (see Fig. 12). In Ref. [76], they described the sensitivity of the seed placement error to changes in physician-controlled parameters such as depth and height of needle insertion, needle sharpness, needle friction, velocity of needle insertion as well as patient-specific parameters such as Young's modulus or tissue stiffness. They concluded that "inserting the needle deeper and/or using sharper needles with less surface friction can decrease seed placement error and that the variances of the biological parameters of global tissue stiffness and compressibility have only a minimal effect on seed placement error" [76]. They also found that increasing needle insertion velocity results in smaller deformation and decreases seed placement error. However, the velocity cannot be set high due to the requirement for path verification during insertion and safety issues [76]. Different algorithms were also compared to increase the accuracy of real-time tissue modeling in Ref. [77].

Heimenz et al. [79] and Holton [80] developed a force feedback model using data obtained from insertion in different materials relevant to epidural insertion. The model was used to drive haptic devices for needle insertion simulation software which was developed for training anesthesiology residents [81].

4. Modeling needle deflection

The problem of needle deflection is one of the reasons for inaccuracy in the needle insertion procedure. During insertion of the needle, the tissue around the needle tip is compressed and the unbalanced resistance force against the compression due to the needle geometry can deflect the needle [16]. Moreover, the thin needle has to pass through layers of tissues with different properties, which would affect the net amount of needle deflection.

Okamura et al. [49] studied the effect of needle geometry on needle bending. Their results showed that needles with smaller diameters and bevel tips lead to more needle bending whereas conical and triangular tips have less bending that is also more consistent. They also noted that "a beveled-tip needle bends because it is asymmetric and receives higher force on one side". However, the reason for bending in a needle with a symmetric-tip (needle with triangular or conical tip) can be the changes in the mechanical properties of the material into which the needle is inserted. Material inconsistency

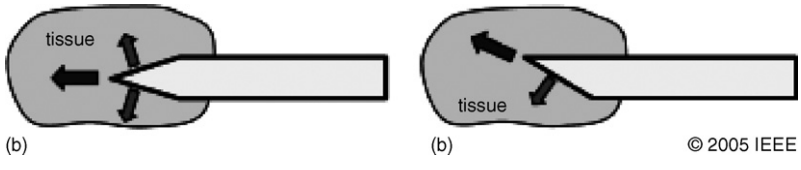

Fig. 13. (a) A symmetric-tip needle exerts forces on the tissue equally in all directions, so cutting the tissue occurs in the moving direction of the needle tip. (b) A bevel-tip needle exerts forces asymmetrically so cutting the tissue occurs at an offset angle depending on the bevel angle, needle flexibility and tissue properties [17].

may also be a reason for inconsistent bending of beveled-tip needles [49]. Fig. 13 shows how a flexible needle with a bevel tip cuts tissue at an angle and causes needle deflection during insertion.

Kataoka et al. [16] proposed a model for force-deflection of a beveled-tip needle during insertion. A physical quantity called infinitesimal force per unit length was used in order to find the amount of needle deflection during insertion. This quantity was adopted from the traction definition $\lim_{\Delta s\to 0} \Delta F_s/\Delta s$ (F is the surface force and s is the area) used in the stress studies [16]. However, due to the long thin shape of the needle, they defined infinitesimal force per unit length as $\lim_{\Delta l\to 0} \Delta F_l/\Delta l$ (ΔF is the force acting on the segment of a deflected needle and Δl is the length of a deflected needle segment). According to the model (see Fig. 14), the needle deflection is described as

$$g(l,d) = \frac{W(d)}{24EI}(l^4 - 4l_{\text{in}}(l_{\text{in}}^2 + 3l_{\text{in}}l_{\text{out}} + 3l_{\text{out}}^2)l + l_{\text{in}}(3l_{\text{in}}^3 + 12l_{\text{in}}^2 l_{\text{out}} + 18l_{\text{in}}l_{\text{out}}^2 + 8l_{\text{out}}^3)), \quad 0 \le l \le l_{\text{in}} \tag{6}$$

where l is the length of the needle, l_{in} and l_{out} the lengths of the needle inside and outside the tissue, respectively, $W(d)$ the force per unit length, d the needle diameter, E Young's modulus for the needle (2.0×10^2 GPa for stainless steel material) and I is the moment of inertia of the needle. They considered $W(d)$ to be constant for needles with the same diameter. Kataoka et al. [16] performed needle insertion into a swine's hip muscle tissue and measured the needle deflection using X-ray imaging. They compared the amount of the measured deflection with the amount predicted by (6). The slope of displacement versus length at different needle diameters was comparable; however, the predicted deflection was smaller than the measured deflection. They suggested that there is another degree of freedom, a moment or rotational component, which accounts for the actual deflection. In their model, the mechanical properties of soft tissue, tissue deformation and the bevel angle of the needle are not considered. It cannot be generalized from their results whether in insertions with the same needle into different tissues, the value of W would still remain the same.

Webster et al. [82] performed needle insertion into a rubber-like simulated muscle. They used needles with different bevel angles. The angles used were 5°, 25°, 40°, 60° and 80° and the insertion depth was 22–25 cm. Their results showed that decreasing the bevel angle increases the amount of needle deflection (bending) but the bevel angle has little impact on the amount of axial force. They also performed insertion with different velocities from 0.5 to 2.5 cm/s. They found that the velocity of needle insertion in homogeneous, relatively stiff phantom tissue had no discernable effect on the amount of needle deflection. From their result, the velocity did change the amount of the axial force. While the result of their study on needle deflection matches with *in vivo* observations, their study on the effect of velocity requires *in vivo* validation. Moreover, inserting a needle 22 cm would certainly deform soft tissue, while in Ref. [82] no macroscopic displacement occurred.

5. Automated needle insertion

5.1. Force sensory data

One of the requirements for precise control of robotic needle insertion is the capability to identify tissue types

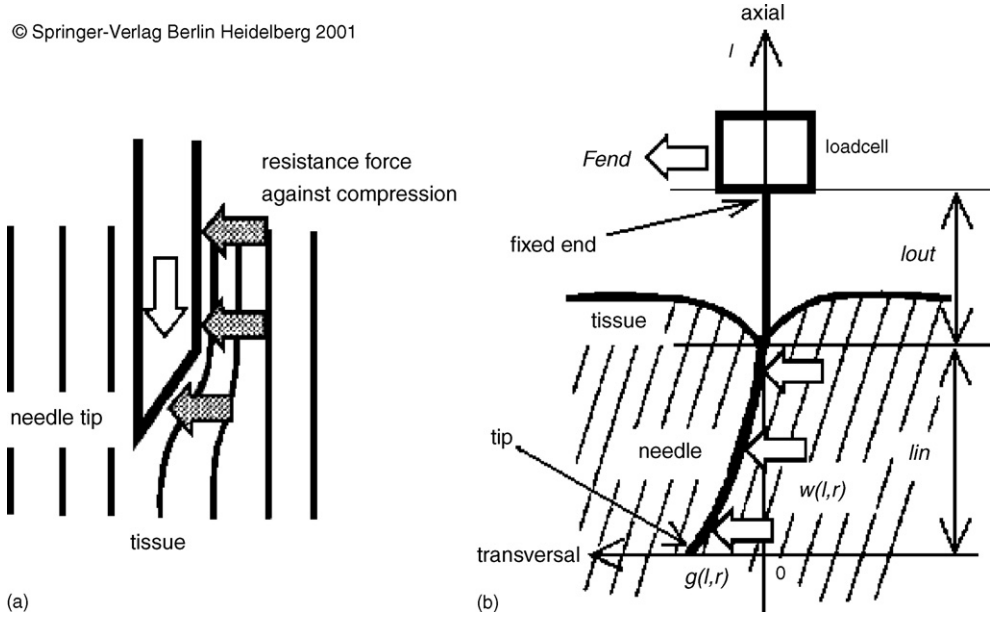

Fig. 14. A force-deflection model for a beveled-tip needle during penetration into soft tissue: (a) force on a needle tip; (b) force and deflection of a needle [16].

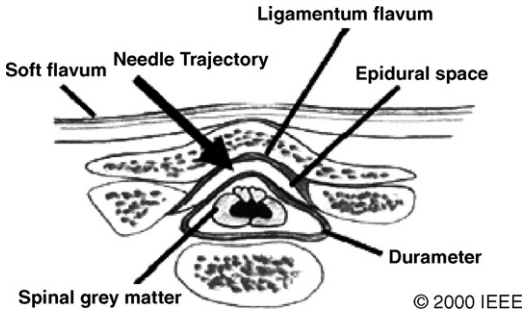

Fig. 15. Location of the epidural space [84].

and their deformation in real time. Brett et al. studied the use of force sensory data for stapedotomy in Ref. [83] and epidural puncture in Ref. [84]. In stapedotomy (a part of the stapedectomy procedure to the middle ear), force sensory data was useful to identify the state of the procedure [83]. In epidural puncture, laser-based spectroscopy and force sensory data were used to identify tissue type and deformation [84]. As defined in Ref. [84], "epidural puncture is the procedure that places an anesthetic locally in the epidural space within the spinal canal surrounding the spinal cord". During this procedure, the needle passes through the skin, fatty tissue, the supraspinous ligament, intraspinous ligament and the tough ligamentum flavum (see Fig. 15). As mentioned in Ref. [84], it is important in this procedure to avoid puncturing the dura surrounding the spinal nerve tissues and fast reaction to a change in tissue resistance is required for accurate needle placement. Brett et al. [84] stated that "tactile sensing alone cannot be used to interpret tissue type". Therefore, a spectroscopic technique was used based on Raman scattering (in which molecular vibrations and rotational transitions, driven by an external field, are measured) as a potential method for determining tissue type. To use the spectroscopic technique intraoperatively, a fiber-optic cable was inserted into a needle and the tissue at the needle tip was continuously identified. This technique is only suitable for procedures with hollow needles.

Shimoga and Khosla [14] studied safe planning and execution of stereotactic neurosurgery. In stereotactic neurosurgery, it is required to have good visualization of the interior of the patient's skull in order to determine tumor location and to find the best path for inserting the surgical probe [14]. It is also crucial to insert the tool into pre-determined locations within the brain of a patient without damaging brain tissue or blood vessels. Shimoga and Khosla [14] defined two sources of possible human error in such operations: inaccurate visualization and lack of force reflection. They proposed a system consisting of a 3D virtual model of the human brain constructed by multimodal medical imaging and a force reflecting insertion device that is remotely controlled by the surgeon. The virtual brain model would display the probe location in real-time during insertion. A practical implementation of the proposed system was not found in the literature.

Washio and Chinzei [85] carried out manual and robotic needle insertion experiments into bovine liver. They found that a force sensor could detect the moment of puncture slightly faster than video-based detection. In addition, they found that a force sensor could be more sensitive than a skilled surgeon for detecting the moment of puncture. Gerovichev et al. [27] evaluated the effect of visual and haptic feedback. Using a virtual needle insertion simulator they studied the detection of puncture of a particular layer with two groups of volunteers. One group had medium exposure to a haptic interface and the virtual environment and low exposure to real needle insertion and the other group had extensive experience in real needle insertion and no experience in haptics. The results in Ref. [27] showed that the addition of force feedback reduces the error in detection of transitions between tissue layers; however, real-time visual feedback provides greater improvement in performance than force feedback.

5.2. Needle insertion techniques

Some researches [17,72] have used the flexibility of the needle during insertion to increase its maneuverability. They refer to this technique as needle steering. Others have studied different trajectories for needle insertion with the aim of reducing needle deflection and tissue deformation.

In Section 3, we discussed the needle insertion model developed by DiMaio and Salcudean [54]. They used a robot with 3 degrees of freedom—translation of the needle base perpendicular to the insertion direction, translation along the insertion direction, and rotation about the insertion axis. In their experiments, they used a needle with a Franseen tip (which was stiff relative to the tissue) in order to avoid the problem of deflection due to a bevel tip. In Ref. [72], DiMaio and Salcudean used their model to study the kinematics of motion-planning and introduced a "needle manipulation Jacobian" for needle steering and manipulation. The Jaco-

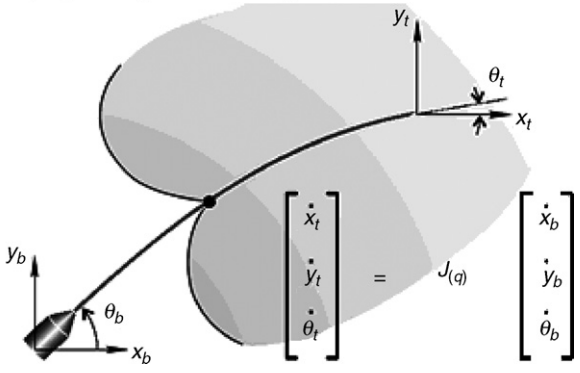

Fig. 16. Steering and the *needle manipulation Jacobian* [72].

bian is defined by the relationship between the needle tip and the base velocities (see Fig. 16):

$$J = \left[\begin{bmatrix} \frac{\partial x_t}{\partial x_b} & \frac{\partial x_t}{\partial y_b} & \frac{\partial x_t}{\partial \theta_b} \end{bmatrix} \begin{bmatrix} \frac{\partial y_t}{\partial x_b} & \frac{\partial y_t}{\partial y_b} & \frac{\partial y_t}{\partial \theta_b} \end{bmatrix} \begin{bmatrix} \frac{\partial \theta_t}{\partial x_b} & \frac{\partial \theta_t}{\partial y_b} & \frac{\partial \theta_t}{\partial \theta_b} \end{bmatrix} \right]^{\mathrm{T}} \quad (7)$$

They incorporated soft tissue motion, needle flexibility and a physically based contact model in order to plan the needle trajectory. In their approach, the tissue was moved by steering the needle base outside the tissue and obstacles were avoided. They used a task-space potential field approach and validated their algorithms via simulation (see Fig. 17) and robot-controlled trajectory experiments in a transparent PVC phantom. In Ref. [73], DiMaio and Salcudean discussed the sensitivity of the results of simulation and planning to biomechanical properties of soft tissue. Their results showed that when the Young's modulus was variable from 50% to 150% of its nominal value, the final needle tip placement error increased to 2.5 mm. The simulation was insensitive for this variation with respect to the proximity to obstacles [73].

Similar to the steering technique of DiMaio and Salcudean but with a simplified model for the tissue and flexible needle, Glozman and Shoham [86] performed fast path planning and real-time tracking for the needle in order to avoid an obstacle and hit a target. To simplify the model, they approximated the tissue using virtual springs model and used an inverse kinematics approach to translate and orient the needle base. They found that the needle base trajectory can be varied and can be optimized to minimize the lateral pressure of the needle shaft on the tissue. They decreased both the base stroke and the pressure by relaxing the requirement for the tip orientation to be tangent to the path [86].

In Ref. [87], Webster et al. developed a nonholonomic model for steering flexible bevel-tipped needles in relatively hard tissues. In contrast to the approach presented by DiMaio and Salcudean [72], the needle used in Ref. [87] was flexible relative to the tissue and needle steering did not cause tissue displacement. Choosing stiff material to represent the tissue may not be realistic. However, it is acceptable for preliminary experiments because it allows one to study the effects of needle deflection during needle insertion without the complication of tissue deformation. It should be mentioned that needle deflection could be a function of tissue deformation since the latter can change the direction and magnitude of forces acting on the needle. The device in Ref. [87] provided two degrees of motion: translation in the insertion direction and rotation about the translational axis. Two control inputs were proposed: insertion velocity and rotation velocity, to move the needle to a desired position and orientation. Using the "bicycle-like" nonholonomic model shown in Fig. 18, the kinematic model for the needle tip position can be calculated using:

$$\dot{g}_{\mathrm{ab}}(t) = g_{\mathrm{ab}}(t)(u_1 \hat{V}_1 + u_2 \hat{V}_2);$$
$$n(t) = R_{\mathrm{ab}}(t) l_2 e_3 + p_{\mathrm{ab}}(t) \quad (8)$$

where g_{ab} and R_{ab} are the rigid transformation and the rotation matrices between frames A and B, u_1 and u_2 insertion and rotation speeds, $\hat{V}_1$ and $\hat{V}_2$ Lie representations of total (linear and angular) insertion and rotation velocities, p_{ab} the position of the origin A relative to B, e_3 is calculated using $p_{\mathrm{bc}} = l_1 e_3$, p_{bc} the position of the origin B relative to C, and l_1 and l_2 are as shown in Fig. 18. Although in the bicycle-like nonholonomic model for needle steering proposed in Ref. [87], the speed of needle rotation was incorporated, in their actual experiments, the speed of insertion was constant and needle rotation speed was zero. Their experiments showed that the needle tip followed a circular arc that was a function of the parameters ϕ, l_1 and l_2 which also fit the curvature obtained from the nonholonomic model. The actual control and steering were not performed in the experiments. They identified a problem in controlling the spin of the needle as a result of the finite torsional stiffness of the needle. It should be added that the highly stiff tissue used in their experiments might be another cause of such a problem. The existence of such a problem needs to be investigated with *in vivo* experiments where lubrications (as the result of blood circulation and moisture in the tissue) may play an important role. An analytical relationship between the needle steering angle and the bevel angle is yet to be determined [87].

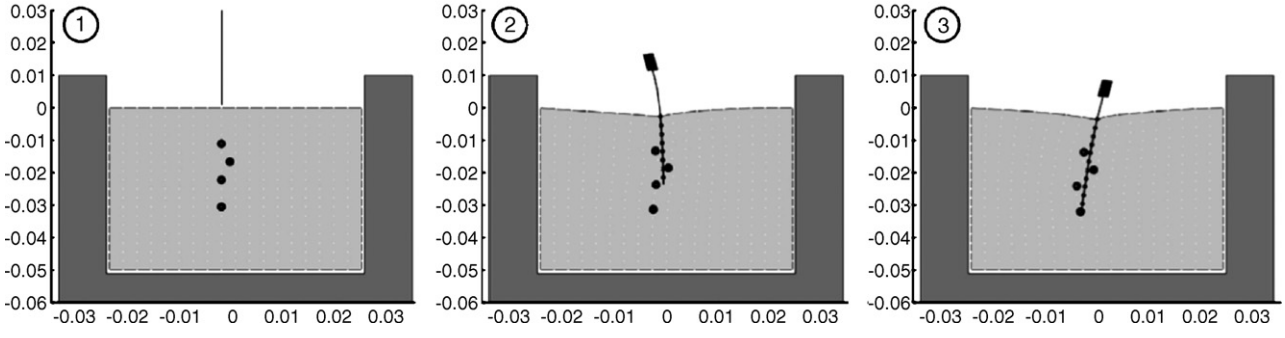

Fig. 17. Simulated needle trajectory plan in an environment containing three obstacles [72].

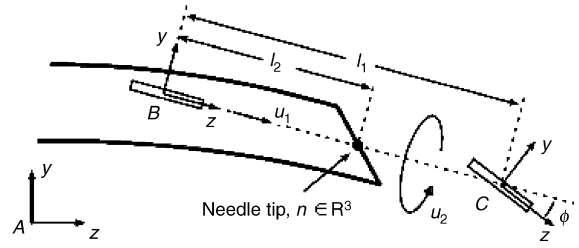

Fig. 18. Configuration of a bevel-tip needle during steering with the superimposed "bicycle-like" nonholonomic model. The front and back wheels at frames B and C are shown. The *x*-axes for all frames are pointing into the page [87].

Alterovitz et al. [29] used their 2D needle insertion simulator (discussed in Section 3) for sensorless planning and needle steering. In Ref. [88], Alterovitz et al. presented a sensorless planning method for radioactive seed implantation in prostate brachytherapy, which combined numerical optimization with soft tissue simulation. The needle offsets were computed to minimize seed placement error by compensating for predicted tissue deformation. In Ref. [17], they used their simulation for steering highly flexible needles with bevel tip into tissues with obstacles. In their simulation, they presented results for needle deflection in rigid and soft tissues. In rigid tissues, the needle follows a path of constant curvature during insertion while in soft tissues the curvature is not constant and depends on tissue properties and the frictional forces between the needle and the soft tissues. Unlike DiMaio and Salcudean [72,73], Alterovitz et al. [17] used a numerical optimization technique for steering the needle. The goal was to avoid polygonal obstacles, minimize the insertion distance and compensate for simulated tissue deformation. Therefore, the control variables (X) were defined as insertion distance (d), bevel rotation (b), initial position (y_0) and insertion angle (θ). Variables d, y_0 and θ were constrained by the length of the needle ($d_{\max}$), width of the rectal probe ($y_{\max} - y_{\min}$), and $[-45°, 45°]$, respectively. They also defined constraints for the needle distance from the target and the obstacle which were converted to penalty functions [89]. The optimization was separately performed on bevel-right (0°) and bevel-left (180°) states of the needle at each step. They solved the constrained nonlinear optimization problem:

$$\min_X F(X) = d + \mu(\max\{\|p_d - t\| - \varepsilon_t, 0\})^2 + \mu\left(\int_0^d \max\{-c_s + \varepsilon_o, 0\}\,ds\right)^2$$
$$\text{subject to :} \quad y_{\min} \le y_0 \le y_{\max}, \quad \theta_{\min} \le \theta \le \theta_{\max}, \quad 0 \le d \le d_{\max} \tag{9}$$

where p_d denotes the needle tip coordinates, t denotes the target coordinates, ε_t and ε_o tolerances for the needle tip distance from the target and the obstacle, c_s the distance from every node on the needle shaft to the closest obstacle and $s \in [0, d]$ are all nodes along the needle shaft. Similar to their sensorless planning algorithm, Alterovitz et al. [17] found the optimal initial location, orientation and insertion depth based on predicted tissue deformation and then inserted the needle. The simulation results have yet to be compared with physical experiments [17]. One question that may rise is the medical application which avoiding several obstacles during needle insertion is required. None of the papers reviewed have explicitly discussed such medical cases. However, intramediastinal or intra-abdominal biopsies and abscess draining could be examples of medical applications that require such procedures [90–92].

Several experiments have been carried out by researchers using different techniques for inserting needles into soft tissue in order to reduce insertion forces while achieving less tissue deformation and needle deflection. Meiklejohn [93] showed that rotation of an epidural needle significantly decreases the force required to puncture the dura. However, it was recommended that rotation should be applied only during the initial part of needle insertion because after insertion of the tip into the epidural space, there is a likelihood of tearing the dura due to the beveled shape of the needle tip. A few years later, Hochman and Friedman [94] studied the effect of different manual needle insertions on the force necessary to puncture and advance a needle through tissue phantoms for applications in dentistry. They tried a linear insertion technique and a bidirectional rotation–insertion technique on tissue phantoms with different densities and using needles of different gauges. The bidirectional rotation–insertion technique involves insertion while rotating the needle through 180° in each direction about its axis. In their experiments, the needle was moved to a depth of 1.27 cm in 12 s. Their results revealed that bidirectional insertion requires less force for puncturing and penetration than linear insertion irrespective of the material and needle gauge. Interestingly little if any deflection was observed when bidirectional rotation was used in an insertion with a bevel-tip needle.

Abolhassani et al. [95,96] studied the effect of different trajectories on tissue indentation and friction force. They performed experiments on *ex vivo* turkey tissue with its skin intact using a 6-DOF force/torque sensor and a robot with two degrees of freedom—translation in one (horizontal) direction and rotation about the translational axis. A needle with a bevel tip was used for the experiments and the same upward orientation of the bevel tip at the skin contact point was considered. For each constant velocity along the translational axis, the effect of different rotational motions was compared. The following were considered: no rotation, continuous rotation with different speeds, bidirectional rotation with different rotational angles and speeds, and needle rotation based on forces orthogonal to the insertion direction. The results showed that having rotational motion can reduce the amount of tissue indentation as well as the friction force between the needle shaft and the tissue [95]. In the exper-

iments, lateral forces were the result of forces exerted by the tissue on the needle which also cause needle deflection. The results showed that controlling the rotational motion by keeping as close to zero as possible the lateral forces acting on the needle gave the best result among different types of rotational motions. Using an imaging system could provide better validation of these results. In general, physicians tend not to favor needle rotation although it reduces friction forces and makes the insertion procedure easier. The main reason is the increased trauma to the patient in the region of penetration. In their study, Abolhassani et al. [96] also tried different types of translational motions for needle insertion. They showed that an increase in needle insertion velocity to a certain extent could reduce the amount of tissue deformation. They also used the infinitesimal force per unit tissue displacement $K_e = \lim_{\Delta x \to 0}(\Delta f/\Delta x)$ (f is the force acting on the needle and x is the displacement of tissue in the insertion direction) before puncture for updating an online trajectory for needle insertion in order to reduce the amount of tissue indentation. The value of K_e is related to tissue stiffness prior to puncture. They chose a desired K_e at the point of puncture by one insertion with a constant velocity of 10 mm/s. In subsequent insertions, at each time step they calculated the error between the current K_e and the desired K_e and used that error as a gain factor to increase the velocity of the translational motion. Their results showed that a trajectory which combines the rotational method with online update can reduce the amount of tissue indentation by about 20%. The online trajectory method might be useful for applications with multiple needle insertions such as in prostate brachytherapy. However, there are a few issues to be addressed in their work such as *in vivo* experiments to determine the effect of these trajectories, and the effect of the trajectories on tissue deformation after puncture. It should also be mentioned that after puncture tissue slides back on the needle and this affects the net amount of tissue deformation.

6. Challenges

The aim of most of the studies related to needle insertion into soft tissue is to increase the accuracy of insertion which may help to improve the effectiveness of the corresponding therapy or the precision of the diagnosis. While these studies can be carried out independently of the applications, the results obtained have a broader impact in the general area of percutaneous intervention or therapy. For example, while modeling soft tissue using accurate mechanical properties is required for developing realistic training simulators, it also contributes towards improving trajectory planning and treatment strategies for actual surgeries. Much of the research in this area is still in its early stages and considerable research needs to be done before acceptable or desirable performance is achieved. In the following sections, we summarize the current state of research and discuss future directions.

6.1. Analytical modeling

Needle insertion forces consist of stiffness force, cutting force and friction force distributed along the needle shaft. Analytical models are suggested for these forces and they can be considered as providing the foundation on which to base improvements and validation for different tissue types. For more accurate models, patient-specific parameters (e.g., age, gender), vascular pressure, bleeding and temperature [49] should be investigated in addition to the type of tissue into which the needle is inserted.

The models used for tissue modeling are currently limited to mass-spring and finite elements. They are mainly linear, homogeneous models. Research needs to be focused on developing complex, real-time models that incorporate nonlinearity, inhomogeneity, anisotropy and viscosity of *in vivo* tissues. To improve the computational efficiency of FEM employed in simulations, the use of parallel algorithms and multi-processor systems should be extended to needle insertion simulations. Artificial neural networks may provide another approach for modeling soft tissues because of their potential for modeling extremely complex systems. The universal approximation ability, the parallel network structure and the availability of online and off-line learning methods are some properties that make artificial neural network a good tool for tissue modeling. When modeling an organ, it is also important to consider the anatomy of that organ and surrounding tissue types because all these can affect access to the target and organ deformation during the procedure. The anatomy of an organ defines the shape of an organ, its location and surrounding tissue layers that a needle is required to pass through in order to reach the target. Ref. [97] is an example of studies on the effect of surrounding tissue on deformation and force sensation.

Several research groups have tried to model needle deflection during insertion; however none of the available models integrate mechanical properties of soft tissue. The shape of the needle tip is also a parameter to be considered in modeling needle deflection and current studies are now focused on this aspect.

6.2. Experimental studies

Mechanical properties of *in vivo* soft tissue are very important in simulation and modeling. A few devices have been developed to measure stress/strain, indentation and stiffness *in vivo*. Nevertheless, developing tools that are able to measure different properties for different organs is still of much research interest. Creating a standard database that provides data on the variation of mechanical properties would be very useful. In such database, it is important to differentiate between tissues from different patients (age and gender matter) and different organs. Also it should be noted that mechanical properties vary between healthy, damaged and diseased tissues. Such a database could help to define parameters of analytical models.

One of the best methods to gather data is to use tools equipped with force sensors and obtain imaging data during actual procedures [55]. This can help to obtain large amounts of *in vivo* data for more complete analysis and modeling.

6.3. Robotics and control

Needle insertion is one of the medical applications that can benefit from advances in the field of robotics in general and medical robotics in particular. An unprecedented amount of interest has been shown in recent years for autonomous needle guidance and steering. Much emphasize has recently been placed on needle steering in order to avoid obstacles, minimize tissue deformation and reach the anatomical region that is not accessible using straight-line trajectory. However, no control strategy has yet been suggested for autonomous needle insertion that can be used as a reference or as a basis for comparison.

Most of the current studies on modeling and planning needle insertion are performed using artificial phantoms such as silicon based materials. Although these phantoms are relatively easy to construct and their results are usually reproducible, to the best of our knowledge, there is currently no artificial phantom available that shows the complex behavior of soft animal tissue. There are many problems that need to be addressed with regard to building nonlinear thick phantoms or multi-layer thin phantoms. The result of the studies mentioned in Sections 6.1 and 6.2 (analysis and modeling of patient-specific tissue deformation) show a direct effect on control and guidance of the needle during insertion. Flexibility and shape of the needle tip are factors which require special attention in trajectory generation for needle insertion.

Using master–slave robots, incorporating haptics and developing appropriate and effective haptic devices is another area of research which may be useful for needle insertion. There are two major benefits in master–slave operations. First, the needle can be controlled by a surgeon; therefore the surgeon's expertise is in the loop. Second, the slave motions can be restricted using virtual fixtures.[2] Therefore, it should be possible to achieve significantly greater accuracy than that in a conventional procedure. Also, haptics can provide a means of introducing realism in simulators for needle insertion training. Although teleoperated procedures can benefit from the addition of force feedback [99,100] (especially when the quality of imaging is not good), it is known that real-time imaging feedback of sufficiently good quality is a more effective aid than haptic feedback alone [27].

6.4. Software systems and imaging

Development of reliable software systems for simulation and planning requires enterprise architecture and multi-tier design. In addition, for monitoring and control of robotically assisted needle insertions, working with real-time operating systems plays an important role. Simulation fidelity should be carefully studied in validating medical training software packages. Quantitative fidelity is of special importance in medical simulation. Current heuristic data used in simulation systems should be replaced with analytical models. The disease progression, the procedure, the tool to be used, the physician, active elements, passive elements and interactive elements should be considered in a simulation [101].

Imaging may be used for validating models and experimental results. In percutaneous procedures, one cannot overemphasize the need for real-time imaging (ultrasound, CT, or MRI) for use in tracking and guiding the needle or catheter particularly in autonomous or semi-autonomous procedures. Ultrasound has attracted special attention in the field of needle insertion because not only it is a safe and affordable imaging modality; it also provides information related to tissue properties (elastography), target displacement and tool position. The information can be combined to improve prediction for planning and to reduce target error. Developing 3D and 4D real-time systems for elastic registration and data fusion is an active area of research for different clinical applications.

7. Concluding remarks

In this paper, we have conducted a detailed survey of the research to date concerning needle insertion in soft tissue. In particular, we have examined the role played by tissue deformation, needle deflection and tool–tissue interaction forces. Several techniques for needle guidance and steering were described, and challenges and areas for future research were discussed.

All recent studies show that the axial force of a needle during insertion in soft tissue is the summation of different forces distributed along the needle shaft. Physical phenomena such as cutting/fracture, sliding, tissue deformation and displacement contribute to the variation of forces acting on the needle during insertion [102]. During needle insertion, the moment of puncture can be identified by a sharp drop in the amount of the axial force [49,95]. Friction forces increase as the needle penetrates deeper into tissue [52]. Force data in some procedures have been used for identifying tissue layers as the needle is inserted. It has also been observed that less force is required to puncture and penetrate tissue using robotic insertion than using manual insertion. Different techniques and trajectories have been considered in order to insert needles more accurately with less tissue deformation. It is shown that rotational motion of the needle about its translational axis reduces insertion forces as well as tissue deformation in manual and robotic procedures. Needle deflection and tissue deformation are major problems for accurate needle insertion and they have been extensively studied through simulations and real-time applications. Experiments carried out by different groups have shown that robotic needle insertion can

[2] A virtual fixture is a control aid to limit the motion of a tool to a predefined range or assist the user in moving a tool on a desired path [98].

lead to safer and more accurate needle insertions. With the rapid development of robotic systems, in the very near future, it should be possible to develop very realistic simulations and robotic tools that will enable surgeons to practice needle insertion for appropriate surgeries and therapies. This should reduce trauma to patients, ease the task of surgeons and provide better treatment at lower cost.

Acknowledgements

This work was supported by funds from the Natural Sciences and Engineering Research Council (NSERC) of Canada under a Collaborative Health Research Projects Grant #262583-2003, the Ontario Research and Development Challenge fund under Grant 00-May-0709, and by infrastructure grants from the Canada Foundation for Innovation awarded to the University of Western Ontario and Canadian Surgical Technologies & Advanced Robotics (CSTAR). Financial support for Ms. Abolhassani was provided by an NSERC Postgraduate Scholarship. We would also like to thank IEEE Intellectual Property Rights Office, Springer Science and Business Media and all authors for their kind permission to use figures from their articles in this paper.

References

[1] Bishoff JT, et al. RCM-PAKY: clinical application of a new robotic system for precise needle placement. J Endourol 1998;12:82.
[2] Zivanovic A, Davies BL. A robotic system for blood sampling. IEEE Trans Inform Technol Biomed 2000;4(1):8–14.
[3] Rizun PR, et al. Robot-assisted neurosurgery. Semin Laporasc Surg 2004;11(2):99–106.
[4] Wei Z, Wan G, Gardi L, et al. Robot-assisted 3D-TRUS guided prostate brachytherapy: system integration and validation. Med Phys 2004;31(3):539–48.
[5] Youk JK, et al. Missed breast cancers in ultrasound-guided 14-gauge core needle biopsy: how to reduce them. In: Proceedings of the radiology society of North America events. 2005.
[6] Nath S, et al. Dosimetric effects of needle divergence in prostate seed implant using 125I and 103Pd radioactive seeds. Med Phys 2000;27(5):1058–66.
[7] Rampersaud YR, et al. Application-specific accuracy requirements for image guided spinal surgery. In: Proceedings of the symposium of fourth computer assisted orthopaedic surgery. 1999.
[8] Carr JJ, et al. Stereotactic localization of breast lesions: how it works and methods to improve accuracy. RadioGraphics 2001;21: 463–73.
[9] Roberson PL, et al. Source placement error for permanent implant of the prostate. Med Phys 1997;24(2):251–7.
[10] Hussain HK, et al. Imaging-guided core biopsy for the diagnosis of malignant tumors in pediatric patients. Am Roentgen Ray Soc 2001;176:43–7.
[11] Taschereau R, et al. Seed misplacement and stabilizing needles in transperineal permanent prostate implants. Radiother Oncol 2000;55:59–63.
[12] Narayana V, et al. Optimal placement of radioisotopes for permanent prostate implants. Radiology 1996;199:457.
[13] Kohn LT, et al. To err is human: building a safer health system. New York: Nat Acad.; 2000.
[14] Shimoga K, Khosla P. Visual and force feedback to aid neurosurgical probe insertion. In: Proceedings of the IEEE international conference on engineering in medicine and biology. 1994. p. 1051–2.
[15] DiMaio SP, Salcudean SE. Needle insertion modeling and simulation. IEEE Trans Robot Automat 2003;19(5):864–75.
[16] Kataoka H, et al. A model for relations between needle deflection, force, and thickness on needle insertion. In: Proceedings of the medical image computing and computer-assisted intervention (MICCAI). 2001. p. 966–74.
[17] Alterovitz R, et al. Planning for steerable bevel-tip needle insertion through 2D soft tissues with obstacles. In: Proceedings of the IEEE international conference on robotics and automation (ICRA). 2005. p. 1652–7.
[18] Magill J, et al. Multi-axis mechanical simulator for epidural needle insertion. In: Proceedings of the medical image computing and computer-assisted intervention (MICCAI). 2004. p. 267–76.
[19] Maurin B. et al. A new robotic system for CT-guided percutaneous procedures with haptic feedback. In: Proceedings of the international congress on computer assisted radiology and surgery 2004;1268:515–20.
[20] Hagmann E, et al. A haptic guidance tool for CT-directed percutaneous interventions. In: Proceedings of the IEEE international conference on engineering in medicine and biology. 2004. p. 2746–9.
[21] Hong J, et al. An ultrasound-driven needle insertion robot for percutaneous cholecystostomy. Phys Med Biol 2004;49:441–55.
[22] Kronreif G, et al. Robotic guidance for percutaneous interventions. Adv Robot 2003;17(6):541–60.
[23] Shi M, et al. A stereo-fluoroscopic image-guided robotic biopsy scheme. IEEE Trans Contr Syst Technol 2002;10(3):309–17.
[24] Wang X, et al. 3D real-time interactive needle insertion simulation: soft tissue deformable modeling and sensitivity analysis. In: Proceedings of the international congress on computer assisted radiology and surgery 2004;1268:1326.
[25] Ding M, Fenster A. Projection-based needle segmentation in 3D ultrasound images. In: Proceedings of the medical image computing and computer-assisted intervention (MICCAI). 2003. p. 319–27.
[26] Peters TM. Image-guided surgery: from X-ray to virtual reality. Comput Meth Biomech Biomed Eng 2000;4(1):27–57.
[27] Gerovichev O, et al. The effect of visual and haptic feedback on manual and teleoperated needle insertion. In: Proceedings of the medical image computing and computer-assisted intervention (MICCAI). 2002. p. 147–54.
[28] Nienhuys HW, van der Stappen AF. A computational technique for interactive needle insertions in 3D nonlinear material. In: Proceedings of the IEEE international conference on robotics and automation (ICRA). 2004. p. 2061–7.
[29] Alterovitz R, et al. Simulating needle insertion and radioactive seed implantation for prostate brachytherapy. In: Proceedings of the international conference on medicine meets virtual reality. 2003. p. 19–25.
[30] Kyung KK, et al. Force feedback for a spine biopsy simulator with volume graphic model. In: Proceedings of the IEEE international conference on intelligent robotics and systems (IROS). 2001. p. 1732–7.
[31] Miller S, et al. Advances in the virtual reality interstitial brachytherapy system. In: Proceedings of the Canadian IEEE conference on electrical computer engineering. 1999. p. 349–54.
[32] Fichtinger G, et al. Needle insertion in CT scanner with image overlay—cadaver studies. In: Proceedings of the medical image computing and computer-assisted intervention (MICCAI). 2004. p. 795–803.
[33] Riviere CN, et al. Predicting respiratory motion for active canceling during percutaneous needle insertion. In: Proceedings of the IEEE international conference on engineering in medicine and biology. 2001. p. 3477–80.
[34] Patricui A, et al. Automatic targeting method and accuracy study in robot assisted needle procedures. In: Proceedings of the medical image computing and computer-assisted intervention (MICCAI). 2003. p. 124–31.

[35] Cleary K, Nguyen C. State of the art in surgical robotics: clinical applications and technology challenges. Comput Aided Surg 2001;6:312–28.
[36] Taylor RH, Stoianovici D. Medical robotics in computer-integrated surgery. IEEE Trans Robot Automat 2003;19(5):765–81.
[37] Krieger A, et al. Design of a novel MRI compatible manipulator for image guided prostate interventions. IEEE Trans Biomed Eng 2005;52(2):306–13.
[38] Susil RC, et al. System for MR image-guided prostate interventions: canine study. Radiology 2003;228:886–94.
[39] Fichtinger G, et al. System for robotically assisted prostate biopsy and therapy with interactive CT guidance. Acad Radiol 2002;9(1):60–74.
[40] Schneider C, et al. A robotic system for transrectal needle insertion into the prostate with integrated ultrasound. In: Proceedings of the IEEE international conference on robotics and automation (ICRA). 2004. p. 2085–91.
[41] Ebrahimi R, et al. Hand-held steerable needle device. In: Proceedings of the medical image computing and computer-assisted intervention (MICCAI). 2003. p. 223–30.
[42] Maurin B, et al. A parallel robotic system with force sensors for percutaneous procedures under CT-guidance. In: Proceedings of the medical image computing and computer-assisted intervention (MICCAI). 2004. p. 176–83.
[43] Hong J, et al. An ultrasound-driven needle-insertion robot for percutaneous cholecystostomy. Phys Med Biol 2004;49:441–55.
[44] Shimoga KB. A survey of perceptual feedback issues in dexterous telemanipulation. Part I. Finger force feedback. In: Proceedings of the IEEE virtual reality international symposium. 1993. p. 271–9.
[45] Maurin B, et al. *In vivo* study of forces during needle insertions. In: Proceedings of the scientific workshop on medical robotics, navigation and visualization (MRNV). 2004. p. 415–22.
[46] Simone C, Okamura AM. Modeling of needle insertion forces for robot-assisted percutaneous therapy. In: Proceedings of the IEEE international conference on robotics and automation (ICRA). 2002. p. 2085–91.
[47] Simone C. Modelling of needle insertion forces for percutaneous therapies. Master's thesis. Baltimore, MD, USA: Johns Hopkins University; 2002.
[48] Karnopp D. Computer simulation of stick-slip friction in mechanical dynamic systems. Trans ASME J Dyn Syst Meas Contr 1985;107:100–3.
[49] Okamura AM, et al. Force modeling for needle insertion into soft tissue. IEEE Trans Biomed Eng 2004;51(10):1707–16.
[50] Maurel W. 3D modeling of the human upper limb including the biomechanics of joints, muscles and soft tissues. PhD thesis. Switzerland: Laboratoire d'Infographie-Ecole Polytechnique Federale de Lausanne; 1999.
[51] Fung YC. Biomechanics—mechanical properties of living tissues. 2nd ed. Springer-Verlag; 1993.
[52] Kataoka H, et al. Measurement of tip and friction acting on a needle during penetration. In: Proceedings of the medical image computing and computer-assisted intervention (MICCAI). 2002. p. 216–23.
[53] Matsumiya K, et al. Analysis of forces during robotic needle insertion to human vertebra. In: Proceedings of the medical image computing and computer-assisted intervention (MICCAI). 2003. p. 271–8.
[54] DiMaio SP, Salcudean SE. Interactive simulation of needle insertion models. IEEE Trans Biomed Eng 2005;52(7):1167–79.
[55] Podder TK, et al. Evaluation of robotic needle insertion in conjunction with in vivo manual insertion in the operating room. In: Proceedings of the IEEE international workshop on robot and human interactive communication. 2005. p. 66–72.
[56] Cotin S. Surgical simulation and training: the state of the art and need for tissue models. In: Proceedings of the IEEE workshop on intelligent robotics and systems. 2003.
[57] Parker KJ, et al. Tissue response to mechanical vibrations for sonoelasticity imaging. J Ultrasound Med Biol 1990;16(3):241–6.
[58] Nava A, et al. Determination of the mechanical properties of soft human tissues through aspiration experiments. In: Proceedings of the medical image computing and computer-assisted intervention (MICCAI). 2003. p. 222–9.
[59] Nightingale KR, et al. Investigation of real-time remote palpation imaging. In: Proceedings of the SPIE conference on medical imaging. 2001. p. 224–9.
[60] Trahey GE, et al. Arterial stiffness measurements with acoustic radiation force impulse imaging. In: Proceedings of the SPIE conference on medical imaging. 2003. p. 346–52.
[61] Han L, et al. A novel ultrasound indentation system for measuring biomechanical properties of *in vivo* soft tissue. J Ultrasound Med Biol 2003;29(6):813–23.
[62] Menciassi A, et al. Force sensing microinstrument for measuring tissue properties and pulse in microsurgery. IEEE/ASME Trans Mechatron 2003;8(1):10–7.
[63] Ottensmeyer M, et al. The effects of testing environments on the viscoelastic properties of soft tissues. In: Proceedings of Medical Simulation: Intl Symp ISMS 2004;3078:9–18.
[64] Ottensmeyer MP. TeMPeST 1-D: an instrument for measuring solid organ soft tissue properties. Exp Tech 2002;26(3):48–50.
[65] Brouwer I, et al. Measuring in vivo animal soft tissue properties for haptic modeling in surgical simulation. In: Proceedings of the international conference on medicine meets virtual reality. 2001. p. 69–74.
[66] Brown JD, et al. In-vivo an in-situ compressive properties of porcine abdominal soft tissues. In: Proceedings of the international conference on medicine meets virtual reality. 2003. p. 26–32.
[67] Kerdok AE, et al. Truth cube: establishing physical standards for real time soft tissue simulation. In: Proceedings of the international workshop on deformable modeling and soft tissue simulation. 2001.
[68] Kerdok AE, et al. Truth cube: establishing physical standards for soft tissue simulation. Med Image Anal 2003;7:283–91.
[69] Howe RD. The truth cube: establishing standards for soft tissue modeling. In: Proceedings of the IEEE workshop on intelligent robotics and systems. 2003.
[70] Zienkiewicz OC, Taylor RL. The finite element method. London: McGraw-Hill; 1989.
[71] Cotin S, et al. Geometrical and physical representations for a simulator of haptic surgery. In: Proceedings of the international conference on medicine meets virtual reality. 1996. p. 139–50.
[72] DiMaio SP, Salcudean SE. Needle steering and model-based trajectory planning. In: Proceedings of the medical image computing and computer-assisted intervention (MICCAI). 2003. p. 33–40.
[73] DiMaio SP, Salcudean SE. Needle steering and motion planning in soft tissue. IEEE Trans Biomed Eng 2005;52(6):965–74.
[74] Bro-Nielsen M. Finite element modeling in surgery simulation. Proc IEEE 1998;86(3):490–503.
[75] Nienhuys HW, van der Stappen AF. Interactive needle insertions in 3D nonlinear material. Technical report UU-CS-2003-019. Available: http://www.cs.uu.nl.
[76] Alterovitz R, et al. Needle insertion and radioactive seed implantation in human tissues. In: Proceedings of the IEEE international conference on robotics and automation (ICRA). 2003. p. 1793–9.
[77] Alterovitz R, Goldberg K. Comparing algorithms for soft tissue deformation: accuracy metrics and benchmarks. Technical draft. UC Berkeley: Alpha Lab.; 2002.
[78] Krouskop TA, et al. Elastic moduli of breast and prostate tissues under compression. Ultrason Imag 1998;20(4):260–74.
[79] Heimenz L, et al. Development of the force-feedback model for an epidural needle insertion simulator. J Stud Health Technol Inform 1998;50:272–7.
[80] Holton LL. Force models for needle insertion created from measured needle puncture data. J Stud Health Technol Inform 2001;81:180–6.
[81] Meiklejohn BH. The effect of an epidural needle. An *in vitro* study. Anaesthesia 1987;42(11):1180–2.

[82] Webster III RJ, et al. Design considerations for robotic needle steering. In: Proceedings of the IEEE international conference on robotics and automation (ICRA). 2005. p. 3599–605.
[83] Brett PN, et al. Automatic surgical tools for penetrating flexible tissues. In: Proceedings of the IEEE international conference on engineering in medicine and biology. 1995. p. 264–70.
[84] Brett PN, et al. Schemes for the identification of tissue types and boundaries at the tool point for surgical needles. IEEE Trans Inform Technol Biomed 2000;4(1):30–6.
[85] Washio T, Chinzei K. Needle force sensor, robust and sensitive detection of the instant of needle puncture. In: Proceedings of the medical image computing and computer-assisted intervention (MICCAI). 2004. p. 113–20.
[86] Glozman D, Shoham M. Flexible needle steering and optimal trajectory planning for percutaneous therapies. In: Proceedings of the medical image computing and computer-assisted intervention (MICCAI). 2004. p. 137–44.
[87] Webster III RJ, et al. Nonholonomic modeling of needle steering. In: Proceedings of the ninth international symposium on experimental robotics. 2004.
[88] Alterovitz R, et al. Sensorless planning for medical needle insertion procedures. In: Proceedings of the IEEE international conference on intelligent robotics and systems (IROS). 2003. p. 3337–43.
[89] Bazaraa MS, et al. Nonlinear programming: theory and algorithms. 2nd ed. John Wiley & Sons Inc.; 1993.
[90] Gupta P, et al. Pulmonary arteriovenous malformations: effects of embolization on right-to-left shunt, hypoxemia, and exercise tolerance in 66 patients. Am Roentgen Ray Soc 2002;179:109–12.
[91] Gupta S, et al. Image-guided percutaneous biopsy of mediastinal lesions: different approaches and anatomic considerations. RadioGraphics 2004;24:175–89.
[92] Maher MM, et al. The inaccessible or undrainable abscess: how to drain it. RadioGraphics 2004;24:717–35.
[93] Meiklejohn BH. The effect of an epidural needle. An *in vitro* study. Anaesthesia 1987;42(11):1180–2.
[94] Hochman MN, Friedman MJ. An *in vitro* study of needle force penetration comparing a standard linear insertion to the new bidirectional rotation insertion technique. J Quintessence Intl 2001;32(10):789–96.
[95] Abolhassani N, et al. Experimental study of robotic needle insertion in soft tissue. Proceedings of the international congress on computer assisted radiology and surgery 2004;1268:797–802.
[96] Abolhassani N, et al. Trajectory generation for robotic needle insertion in soft tissue. In: Proceedings of the IEEE international conference on engineering in medicine and biology. 2004. p. 2730–3.
[97] Kuroda Y, et al. Interaction model between elastic objects for haptic feedback considering collisions of soft tissue. Comput Meth Programs Biomed 2005;80(3):216–24.
[98] Abbott JJ, et al. Steady-hand teleoperation with virtual fixtures. In: Proceedings of the IEEE international workshop on robot and human interactive communication. 2003. p. 145–51.
[99] Wagner C, et al. The role of force feedback in surgery: analysis of blunt dissection. In: Proceedings of the 10th symposium on haptic interfaces for virtual environment and teleoperator systems. 2002. p. 73.
[100] Tavakoli M, et al. Robotic suturing forces in the presence of haptic feedback and sensory substitution. In: Proceedings of the IEEE conference on control applications. 2005. p. 1–6.
[101] Issenberg SB, et al. Features and uses of high-fidelity medical simulations that lead to effective learning. Med Teacher 2005;27(1): 10–28.
[102] Brett PN, et al. Simulation of resistance forces acting on surgical needles. J Inst Mech Eng 1997;211(H):335–47.